Independent Component Analysis를 이용한 의료영상의 자동 분할에 관한 연구

論 文
52D-1-10

A Study of Automatic Medical Image Segmentation using Independent Component Analysis

裵 秀 賢* · 兪 善 國** · 金 南 鉉***
(Soohyun Bae · Sunkook Yoo · Namhyun Kim)

Abstract - Medical image segmentation is the process by which an original image is partitioned into some homogeneous regions like bones, soft tissues, etc. This study demonstrates an automatic medical image segmentation technique based on independent component analysis. Independent component analysis is a generalization of principal component analysis which encodes the higher-order dependencies in the input in addition to the correlations. It extracts statistically independent components from input data.

Use of automatic medical image segmentation technique using independent component analysis under the assumption that medical image consists of some statistically independent parts leads to a method that allows for more accurate segmentation of bones from CT data.

The result of automatic segmentation using independent component analysis with square test data was evaluated using probability of error(PE) and ultimate measurement accuracy(UMA) value. It was also compared to a general segmentation method using threshold based on sensitivity(True Positive Rate), specificity(False Positive Rate) and mislabelling rate. The evaluation result was done statistical Paired-t test. Most of the results show that the automatic segmentation using independent component analysis has better result than general segmentation using threshold.

Key Words : Segmentation, Independent Component Analysis, Medical Image, Statistically independent component

1. Introduction

The properties of medical images like Computed Tomography(CT), Magnetic Resonance Image(MRI) over other diagnostic imaging modalities are their high spatial resolution and excellent discrimination of soft tissues, bones and other internal organs. These kind of medical images provide rich information about anatomical structure and enable quantitative pathological or clinical studies; the derivation of computerized anatomical atlases; as well as pre- and intra-operative guidance for therapeutic intervention.

Advanced applications that use the morphologic contents of medical images frequently require segmentation of the imaged volume into each organ types and segmentation of medical images is a prerequisite for a variety of image analysis and visualization tasks. Medical image segmentation is often performed by commercial software using existing algorithms such as region growing, thresholding, boundary detection, and morphological filtering[1]-[6]. However, incomplete segmentation frequently occurs because of several difficulties. First, partial volume artifacts leads to ambiguous boundaries and mixed voxels. Second, adjacent structures connected to the medical images have similar intensity values and make it difficult to separate one structure easily from other interconnected structures.

The manual modification method is the most common way of segmentation in cases of incomplete automatic segmentation[2]-[5][7]. But it is a time-consuming and tedious task because extensive user interaction is involved to modify the incorrectly segmented border on each sectional image. It also requires experienced users to carefully define the features on medical images because of the complexity of that ones. Nevertheless, resultant rendered surfaces still appear uneven. Even though the results of done by the experienced users don't have the consistency.

In this paper, we propose a new automatic approach to segment the features from medical images using Independent Component Analysis(ICA). Independent

* 準 會 員 : 延世大學 醫學工學教室 · 工博
** 正 會 員 : 延世大學 醫學工學教室 副教授 · 工博
*** 準 會 員 : 延世大學 醫學工學教室 副教授 · 工博
接受日字 : 2002年 9月 25日
最終完了 : 2002年 10月 28日

component analysis decompose each signal of an ensemble into components(also called 'basis vectors') that are as independent as possible by a linear transformation of the signals[8]-[10]. The amplitude of a particular component is extracted by a corresponding weight vector(also called a 'filter'[8]). Using this kind of characteristics of independent component analysis, we propose a new automatic algorithm to segment medical images.

2. Independent Component Analysis

The goal of independent component analysis is to recover independent sources given only sensor observations that are linear mixtures of independent source signals[11]. It is a way to find some weigh vector which make the resulting signals are as statistically independent from each other as possible. It is a generalization of principal component analysis that separates the high-order dependencies in the input, in addition to the second-order dependencies[12]. But principal component analysis is a way of encoding second-order dependencies in the data by rotating the axes to correspond to directions of maximum covariance.

Assume two events A and B. Then two events A and B are called independent if

$$P(AB)=P(A)P(B) \tag{1}$$

The conditional probability $P(B \mid A)$ is given by

$$P(B \mid A)=\frac{P(AB)}{P(A)}, \tag{2}$$

and the independence can show that $P(B \mid A)=P(B)$, if $P(A)\neq 0$.

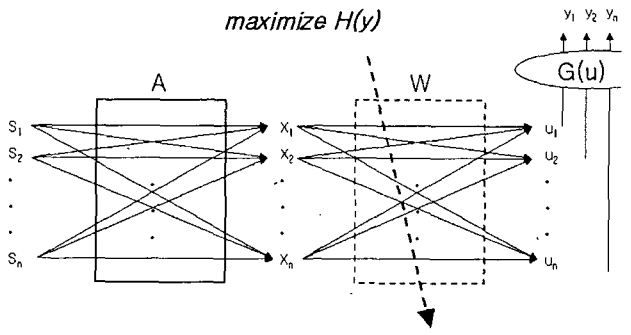

Fig. 1 The instantaneous mixing and unmixing model

Assume that like in Figure 1, we have an input signal X, which is composed of some mixed source signals and the mixing process A and any prior information about the input signal are unknown. If the probabilities of the output signals Y can be made to satisfy Eg. (1), the output signals are independent components of the input signal and we have the mixing matrix $A=W^{-1}$.

Making the output signals as independent as possible is the goal of independent component analysis and it can be accomplished by maximizing the mutual information of the output signals. The mutual information between X and Y is the sum of marginal entropies minus the joint entropy. This is defined as

$$\begin{aligned} I(Y,X) &= H(X)+H(Y)-H(X,Y) \\ &= H(X)-H(X \mid Y) \\ &= H(Y)-H(Y \mid X) \end{aligned} \tag{3}$$

where X is the input, Y is the output and $H(Y)$ is the entropy of the output, while $H(Y \mid X)$ is whatever entropy the output has which didn't come from the input[10]. Entropy is defined as

$$H(X)=\sum_{x\in X} P(x)\log\frac{1}{P(x)}, \tag{4}$$

where the ensemble X is a random variable x with a set of possible outcomes. For $P(x)=0$, the entropy is zero by definition. $H(X)$ is always greater or equal to zero. $H(X,Y)$ is the joint entropy of two variables, interpreted as the redundancy between X and Y or, alternatively, as the reduction in uncertainty of one variable(e.g. X) due to the observation of the other variable Y.

The basic problem of independent component analysis is how to maximize the mutual information that the output Y of a neural network processor contains about its input X. To solve the problem, we consider here only the gradient of information theoretic quantities with respect to some parameter, ω, and assume that Y is the function of ω, in our network

$$\frac{\partial}{\partial\omega} I(Y,X)=\frac{\partial}{\partial\omega} H(Y) \tag{5}$$

because $H(Y \mid X)$ does not depend on ω. This can be seen by considering a system which avoids infinities:

$$Y=G(X)+N, \tag{6}$$

where G is a nonlinear squashing function and N is additive noise on the outputs. In this case $H(Y \mid X)=H(N)$[13].

3. MEDICAL IMAGE SEGMENTATION USING INDEPENDENT COMPONENT ANALYSIS

In this section I describe the method of automatic medical image segmentation using independent component analysis algorithm. To verify the performance of the medical image segmentation using independent component analysis, computer simulations were done with a test data and the medical image data set. The data set in this experiment consists of 27 axial CT images of patient's head, starting from images below chin and ending at images in the upper portion of the nose. The original image data were obtained using a General Electric High-speed Advantage Computerized Tomography under the condition of 120 kVp and 200mA. No special post-processing was performed on the image data, other than that of reducing the bit resolution, 8bits/pixel for efficient memory usage. Figure 2 shows some selected original images from the data set. It is possible to assume that the data set consists of three parts, bone, soft tissue and background, and the final goal of my experiment is to extract bone from the data set. Figure 3 shows the flowchart of bone extraction process.

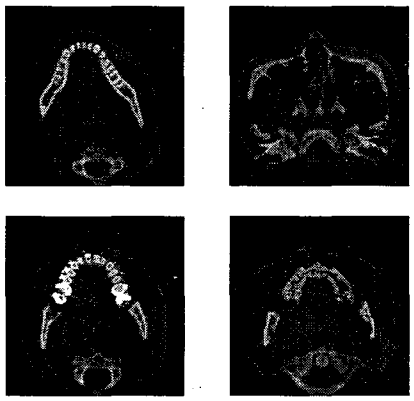

Fig. 2 Selected image data which were used in this experiment

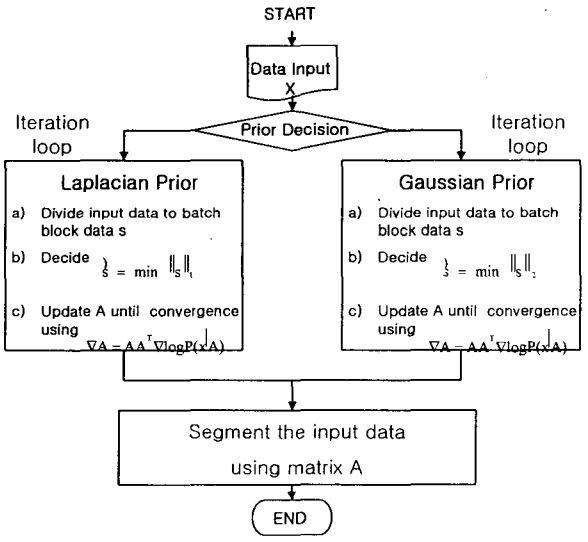

Fig. 3 Flowchart of Medical Image Segmentation Using independent component analysis

It can be assumed that different parts of the medical images have some independent components. In CT images, bone and soft tissue have different attenuation coefficients and this results in different CT number or gray value. In MR images, different relaxation time results in different weighted image. So it is assumed that internal parts of medical image are statistically independent and this is the start of my experiment.

To extract the bone regions from each of the 27 axial image slices, the prior of the data should be decided and it can be decided by the probability density function of the data. The prior can be chosen in terms of the kurtosis of the distribution where the kurtosis is defined as the fourth moment according to Eq. (7).

$$\mathrm{KURTOSIS} = \frac{\sum_i (b_i - \bar{b})^4}{(\sum_i (b_i - \bar{b})^2)^2} - 3 \qquad (7)$$

where $\bar{b}$ is the mean value.

If the kurtosis of the data is zero(Gaussian) or smaller than zero(sub-Gaussian or platykurtic), the Gaussian prior can be chosen and if the kurtosis of the data is larger than zero(super-Gaussian or leptokurtic) the Laplacian prior like in Eq. (8) should be chosen.

$$P(s_m) \propto \exp(-\theta | s_m |) \qquad (8)$$

The super-Gaussian has longer tails and sharper peak than a Gaussian distribution, like Figure 4. Compared to a Gaussian, Laplacian distribution puts greater weight on values close to zero, and as a result the representations are more sparse[14]. After choosing the prior, the data set is iterated using independent component analysis. The goal of this paper is to segment bones and other parts of medical images from one slice and it requires overcomplete matrix. To ensure that the input ensemble was stationary in sequence, the sequence index of the signals was permuted. This means that at each iteration of the training, the independent component analysis training system would receive input from a random sequence index point.

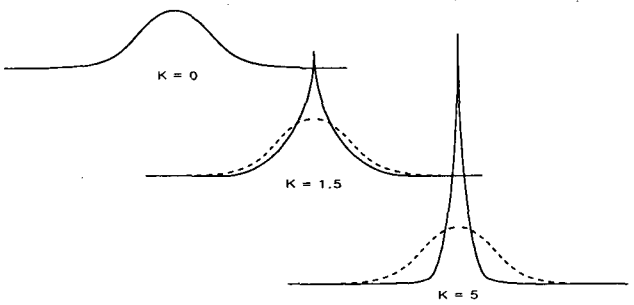

Fig. 4 Examples of three levels of kurtosis. Each of the distributions has the same variance. A Gaussian distribution has minimal redundancy(highest entropy) for a fixed variance. The higher the kurtosis, the higher the redundancy.

In order to evaluate segmentation results of medical image set, SENSITIVITY and SPECIFICITY described in Eq. (9), (10) and other evaluation functions, named Empirical Discrepancy Methods(EDM).

$$\text{SENSITIVITY} = \frac{\sum \text{TRUE}+}{\sum \text{INTRINSIC}+} \tag{9}$$

$$\text{SPECIFICITY} = 1-\frac{\sum \text{FALSE}-}{\sum \text{INTRINSIC}-} \tag{10}$$

In practical segmentation applications, some errors in the segmented image can be tolerated. On the other side, if the segmenting image is complex and the algorithm used is fully automatic, the error is inevitable[15][16]. The disparity between an actually segmented image and a correctly ideally segmented image(reference image) that is the best expected result can be used to assess the performance of algorithm. Both(actually segmented and reference) images are obtained from the same input image. The reference image is sometimes called gold standard.

Weszka and Rosenfeld used an approach to measure the difference between an ideal(correct) image and a segmented image[17]. Under the assumption that the image consists of objects and background each having a specified distribution of gray level, they compute for any given standard segmented value, the probability of misclassifying an object pixel as background, or vice versa. This probability in turn provides an index of segmentation results, which can be used for evaluating segmentation algorithm. In their work, such a probability is minimized in the process of selecting an appropriate segmentation. Recently, a discrepancy measure based on the same principal has been defined. It is termed probability of error(PE). For a two-class problem PE can be calculated by Eq. (11)[18].

$$PE = P(O)\times P(B \mid O) + P(B)\times P(O \mid B) \tag{11}$$

where $P(B \mid O)$ is the probability of error in classifying objects as background. $P(O \mid B)$ is the probability of error in classifying background as objects. $P(O)$ and $P(B)$ are a priori probabilities of objects and background in images. In this case, as the PE value close to 0, the segmentation shows good result.

Image analysis is concerned with the extraction of information from an image, an image yields data out. Here the data are the measurement values of object features obtained from segmented images. One fundamental question in image analysis is whether a measurement made on the objects from segmented images is as accurate as one made on the objects from segmented images. According to this measure, a segmented image has the highest quality if the object features extracted from it precisely match the features in the original. The ultimate goal of image segmentation in the context of image analysis is to obtain measurements of object features. The accuracy of these measurements obtained from the segmented image with respect to the reference image provides useful discrepancy measures. This accuracy can be termed ultimate measurement accuracy(UMA) to reflect the ultimate goal of segmentation. Let R_f denote the feature value obtained from the reference image and S_f denote the feature value measured from the segmented image, the UMA is defined as Eq. (12).

$$\text{UMA} = \frac{|R_f - S_f|}{R_f} \tag{12}$$

As like PE, the UMA value close to 0 means that the result of segmentation is good.

Other evaluation function which is called mislabelling rate described in Eq. (13) are chosen to evaluate the results of segmentation using independent component analysis.

$$F(I) = \sqrt{R}\times \sum_{i=1}^{R} \frac{e_i^2}{\sqrt{A_i}} \tag{13}$$

where I is the image to be segmented, R, the number of regions in the segmented image, A_i, the area, or the number of pixels of the ith region, and e_i, the error of region i[19]. The term $\sqrt{R}$ is a global measure which penalizes small regions or regions with a large error. e_i indicates an appropriate feature whether or not a region is assigned. A large value of e_i means that the feature of the region is not well captured during the segmentation

process. As described in equation (13), the larger value of evaluation function means the bad result of segmentation.

4. RESULT & ANALYSIS

In this section we describe the applications of automatic medical image segmentation using independent component analysis algorithm. To verify the performance of the medical image segmentation using independent component analysis, computer simulations were done with a test data set and 27 axial CT images. The performance evaluations were done using SENSITIVITY, SPECIFICITY, mislabelling rate and EGM which were described in the above.

4.1 Evaluations of Automatic Segmentation with Test Data

This section describes an evaluation of segmentation using independent component analysis. The original data shown in Figure 5 is used. The original data are mixed using a matrix which have 4 random coefficients ranging between 0 and 1. The original data have gray value and is composed of two squares. At first, standard deviations of two squares are set to 35, mean value of large square(Figure 5(a)) is set to 70, and mean value of small square(Figure 5(b))is set to 50. In this experiment the standard deviations of two squares and the mean value of large square are not changed but the mean value of small square is increased by 10 until the mean value of small square becomes 190. Figure 5 shows the selected images of which the mean values are 70(Figure 5(a)) and 130(Figure 5(b)). Figure 5(c) shows the graph of probability density functions when the mean value of large square is 70 and the mean value of small one is 130.

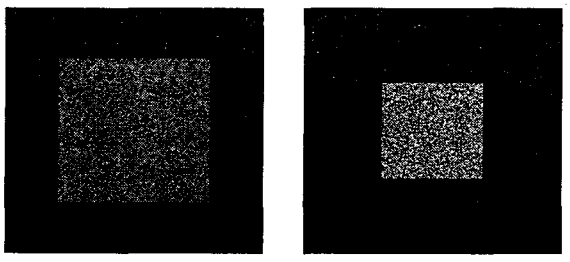

(a) (b)

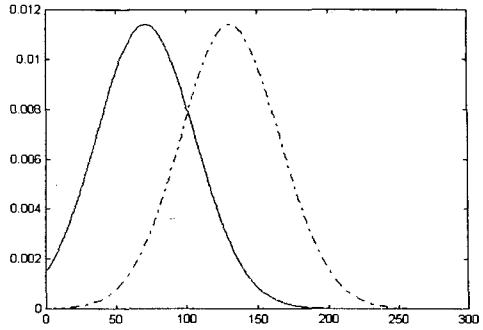

(c)

Fig. 5 The selected original data used in evaluation
(a) Standard deviation 35, mean 70
(b) Standard deviation 35, mean 130
(c) The graph of probability density function

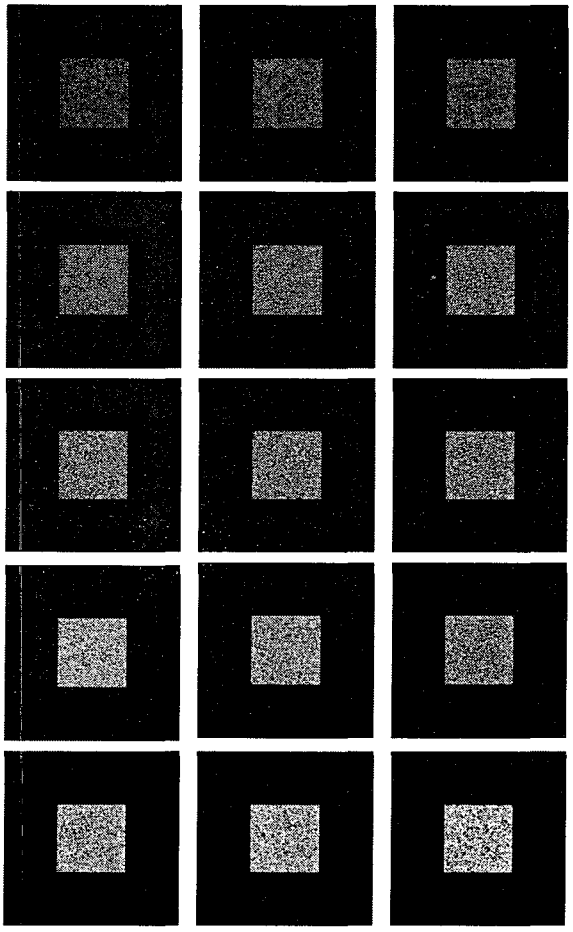

Fig. 6 Small squares extracted from mixed test data

Figure 6 and 7 show the result of segmentation using independent component analysis. The results are ordered by the mean value of small square(Figure 5(b)). Each result shows that the independent component in mixing data can be extracted nearly perfectly. In mixing process, large squares cover all part of small squares. It makes the independent components which represent small squares have some false positive value(Figure 6). But the independent component which represent large squares nearly don't have false positive and true negative values.

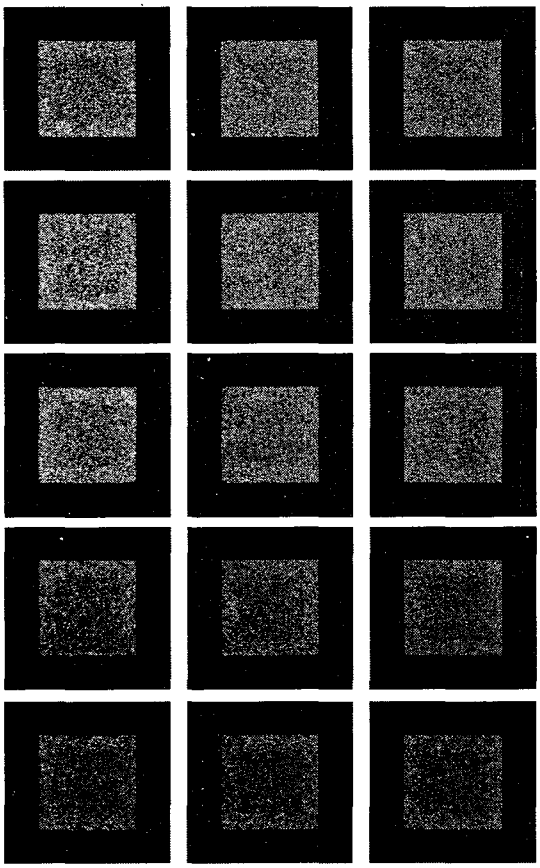

Fig. 7 Large squares extracted from mixed test data

To evaluate the performance of automatic segmentation using independent component analysis, probability of error(PE) and ultimate measurement accuracy(UMA) values which are described in Eq. (11) and (12) are calculated. These values are close to 0 if the results of segmentation are close to original data. Table 1, Figure 8 and 9 show the result of evaluation using PE values and UMA values. All values are close to zero. This means that the segmentation using independent component analysis can extract the independent components from the mixed data and it can be applied to medical image segmentation.

Table 1 Probability of Error and Ultimate Measurement Accuracy value of independent components.

PE Value of Small Squares	UMA Value of Small Squares	PE Value of Large Squares	UMA Value of Large Squares
0.256	0.269	0.092	0.093
0.268	0.254	0.091	0.089
0.297	0.287	0.077	0.075
0.269	0.271	0.064	0.068
0.257	0.263	0.071	0.072
0.257	0.258	0.068	0.067
0.248	0.25	0.068	0.069
0.245	0.248	0.065	0.066
0.237	0.238	0.067	0.065
0.256	0.254	0.094	0.082
0.233	0.241	0.098	0.097
0.278	0.267	0.093	0.095
0.258	0.257	0.094	0.097
0.269	0.264	0.094	0.094
0.231	0.237	0.093	0.091

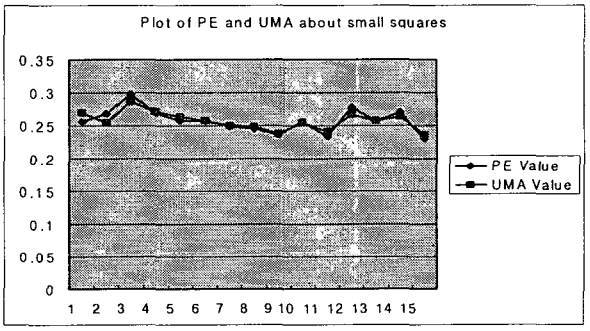

Fig. 8 Plot PE and UMA values about small squares

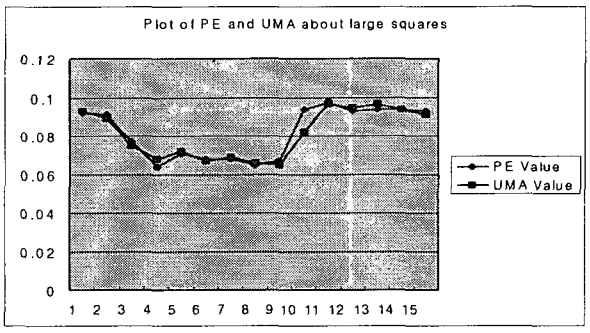

Fig. 9 Plot of PE and UMA values about large squares

4.2 Automatic Segmentation with Medical Images

When segmenting medical images using independent component analysis, the prior of the data set should be chosen. The process of choosing the prior of the data set was done using kurtosis. Figure 10 shows the kurtosis graph and the kurtosis of the data set, respectively.

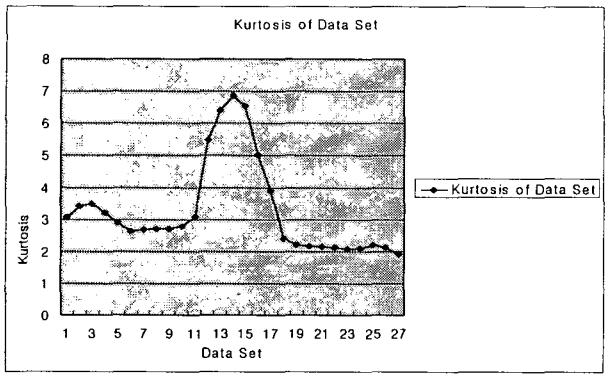

Fig. 10 The kurtosis graph of the input data set. All of the kurtosis are higher than 0, and it means that the input data set have super-Gaussian probability density function.

Figure 11 shows the input image, a slice from a axial view from one slice of the data set. The slice shows chin and cervical spine of female patient and the result of segmentation. Usually the gray value of soft tissue and that of inside the cervical spine are nearly same so it is very difficult to segment the cervical spine exactly using threshold or other method like in Figure 11. Using automatic method which was chosen in this paper, the exact part of chin and cervical spine segmented. Note the significant improvement in the inside area of cervical spine.

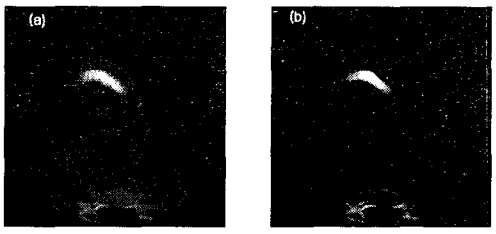

Fig. 11 The input image and the segmentation result.
(a) It is a slice from a axial view from a General Electric High-speed Advantage Computerized Tomography, showing tooth and cervical spine of female patient.
(b) The segmentation result. The tooth and cervical was extracted from (a) except soft tissue.

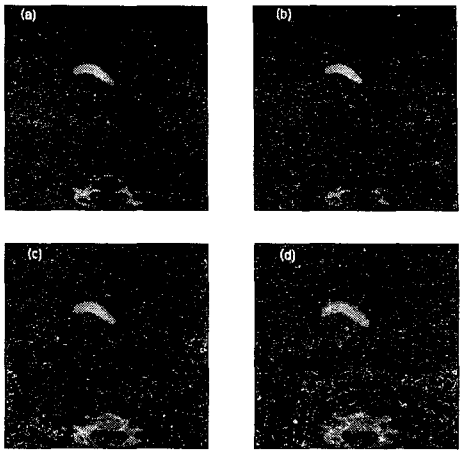

Fig. 12 The segmentation result using threshold. The original image in Fig. 11(a) had gray values. I gradually increased the threshold value and segmented the chin and cervical spine. But the threshold method didn't segment exactly because some parts of the soft tissues and some parts of the cervical spine and chin had same gray values.

In Figure 12(a) and 12(b), inside area of cervical spine is completely absent. In Figure 12(c), inside area of cervical spine is partly absent. In Figure 12(d), inside area of cervical spine has somewhat exact value but the chin has some false positive values and we can not exactly discriminate that part.

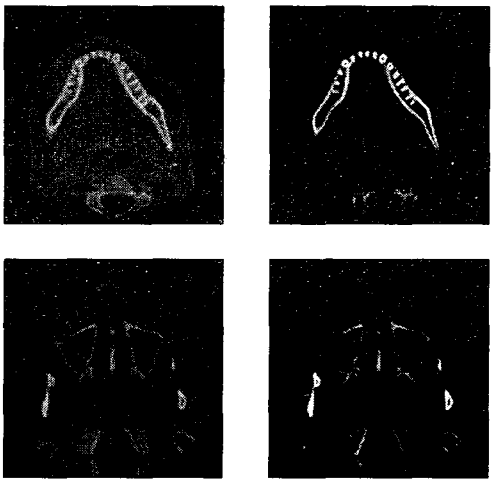

Fig. 13 The segmentation result of CT image. Left images are original CT and right ones are segmented images by automatic method using Independent Component Analysis.

Figure 13 shows the segmentation result of the data set. Left images are original CT and right ones are segmented images by automatic method using Independent Component Analysis. Since bones in CT images have higher gray values than other parts and these are the dominant part of those images, bones are easily segmented using independent component analysis. Figure 14 shows 6 selected axial segmented image using independent component analysis and Figure 15 shows the volume rendering image using the result shown in Figure 14.

4.3 Evaluations of Medical Image Segmentation

This section describes a comparison of segmentation using independent component analysis to segmentation using thresholding method. The manual segmentation results by radiologists was chosen as the reference of a comparison. Figure 16 shows the binary result of manual segmentation. At first the sensitivity comparison was done between independent component analysis method and thresholding method. Sensitivity which is defined in equation (9) shows the "True Positive Rate" of segmented data to reference and higher sensitivity means good segmentation result. Figure 17 shows the result of sensitivity comparison.

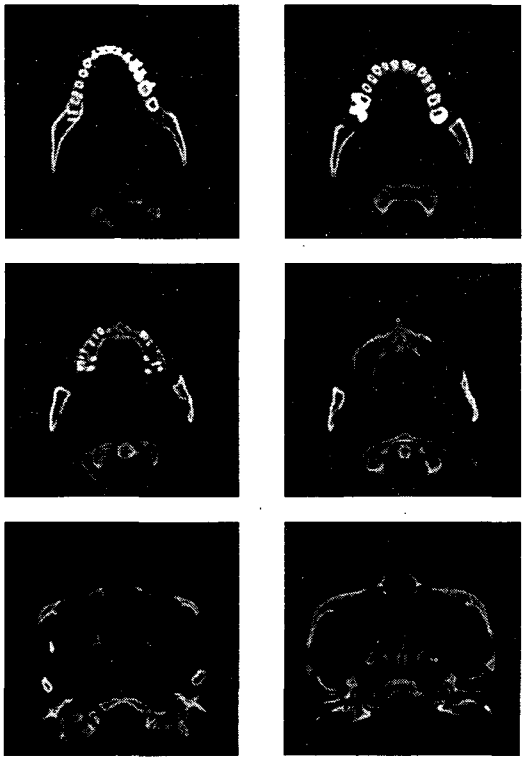

Fig. 14 Result of 6 selected axial CT image segmentation

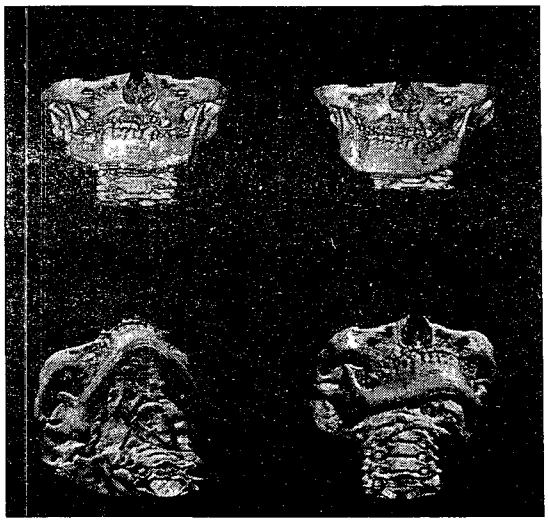

Fig. 15 Volume rendered image using the result of Fig. 14

In Figure 17, the result of 3 image data using independent component analysis out of 27 has lower sensitivity than thresholding method. It is because the 3 image data have tooth and cervical spine and the tooth part have some metal artifacts. The metal artifacts distributed other parts of the soft tissue and this was not segmented clearly using independent component analysis.

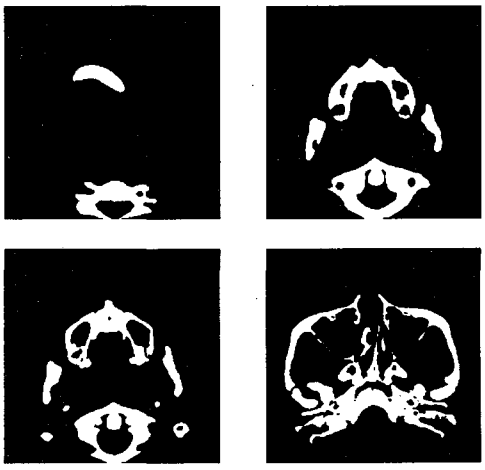

Fig. 16 The result of manual segmentation. These images used as the reference of a comparison segmentation using independent component analysis to segmentation using thresholding method.

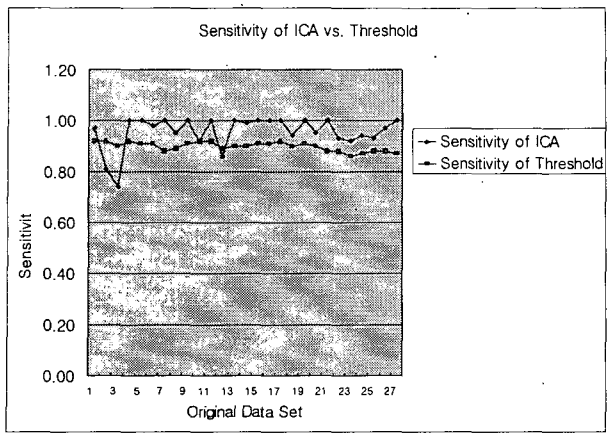

Fig. 17 The sensitivity(True Positivity Rate) comparison between independent component analysis method and thresholding method. The result of 3 image data using independent component analysis out of 27 has lower sensitivity than thresholding method. It is because the 3 image data have tooth and cervical spine and the tooth part have some metal artifacts.

Table 2 The result of Paired-t test about sensitivity with 0.05 statistical significance. p value is much lower than statistical significance. This means that even though the bad result of three cases using independent component analysis, the segmentation using independent component analysis give good results.

	True Positive Rate of Independent Component Analysis	True Positivity Rate of Threshold
Mean	0.982963	0.898519
Variance	0.003691	0.000328
The number of Samples	27	27
Statistically Significance	0.05	
Degree of Freedom	26	
p(T<=t) Value of Paired-t Test	4.8E-07	

A statistical Paired-t test about sensitivity was done using 0.05 statistical significance and p value of Paired-t test was much lower than statistical significance. This means that even though the bad result of three cases using independent component analysis, the segmentation using independent component analysis gave good results. Table 2 shows the result of Paired-t test about the sensitivity.

Secondly the specificity comparison was done. Specificity is defined in equation (10) and 1-specificity shows the "False Positive Rate" of segmented data to reference and lower "False Positive Rate" means good segmentation result. Figure 18 shows the result of "False Positive Rate" comparison. In Figure 18, the result of 6 image data using independent component analysis out of 27 has lower "False Positive Rate" than thresholding method. But other results have nearly same "False Positive Rate". It means that in terms of specificity, the segmentation method using independent component analysis does not have good result comparing to thresholding method. A statistical Paired-t test about "False Positive Rate" shows that the p value of Paired-t test is somewhat higher than statistical significance and it means that there is no significant difference between independent component analysis and thresholding method. Table 3 shows the result of Paired-t test about the sensitivity.

But in Figure 17 and 18, the "True Positive Rate" of independent component analysis is much higher than thresholding method and the "False Positive Rate" is lower and we can infer that the Receiver Operator Characteristic Curve of the independent component analysis method much better shape than the thresholding method. This means that independent component analysis method usually gives better results than thresholding method.

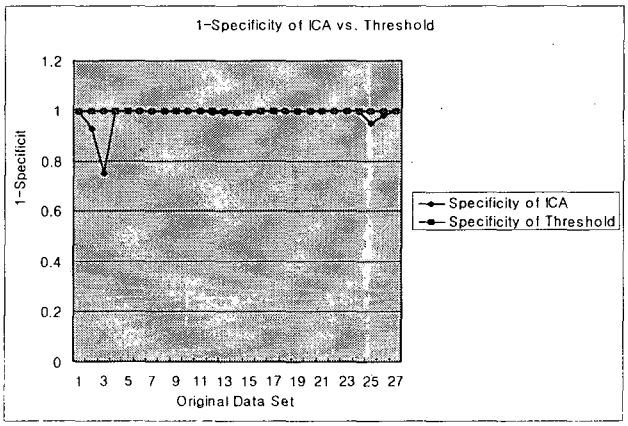

Fig. 18 The result of "False Positive Rate" comparison. The result of 6 image data using independent component analysis out of 27 has lower "False Positive Rate" than thresholding method. But other results have nearly same "False Positive Rate".

Table 3. The result of Paired-t test about "False Positive Rate" with 0.05 statistical significance. p value is higher than statistical significance. It means that there is no significant difference between independent component analysis and thresholding method.

	False Positivity Rate of Independent Component Analysis	False Positivity Rate of Threshold
Mean	0.984074074	0.999259259
Variance	0.00245584	7.12251E-06
The number of Samples	27	27
Statistically Significance	0.05	
Degree of Freedom	26	
p(T<=t) Value of Paired-t Test	0.12460627	

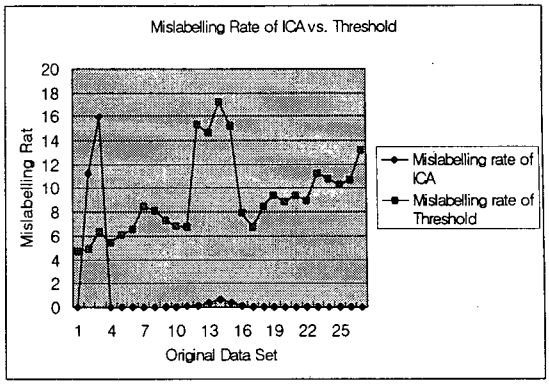

Fig. 19 The result of mislabelling rate comparison. Only 2 cases using independent component analysis out of 27 has higher mislabelling rate than thresholding method. The remainder cases have much smaller mislabelling rate compared to thresholding. It means that although the result of "False Positive Rate" comparison is not good, independent component analysis method will have much good result compared to thresholding method.

At last the mislabelling rate comparison was done between independent component analysis method and thresholding method. Mislabelling rate which is defined in equation (11). This is a combination of the "True Positive Rate" and "False Positive Rate". There is always a trade-off between preserving details and suppressing noise, which is reflected in the evaluation measure the mislabelling rate. If there are too many details in the segmented image, the error of each region may be smaller. But since many small regions are formed and the number of regions is large, the value of mislabelling rate is large which indicates that the segmentation result is not good.

Figure 19 shows the result of mislabelling rate comparison. In Figure 19, only 2 cases using independent component analysis out of 27 has higher mislabelling rate than thresholding method. On the other hand, the remainder cases have much smaller rate compared to thresholding. It means that although the result of "False Positive Rate" comparison is not good, independent component analysis method will have much good result compared to thresholding method. A statistical Paired-t test about mislabelling rate also done using 0.05 statistical significance and p value of Paired-t test was much lower than statistical significance. Table 4 shows the result of Paired-t test about the mislabelling rate.

Table 4. The result of Paired-t test about mislabelling rate with 0.05 statistical significance. p value is higher than statistical significance. This means that although the result of "False Positive Rate" comparison is not good, independent component analysis method will have much good result compared to thresholding method.

	Mislabelling Rate of Independent Component Analysis	Mislabelling Rate of Threshold
Mean	1.069558847	9.254604451
Variance	13.4430021	11.47477914
The number of Samples	27	27
Statistically Significance	0.05	
Degree of Freedom	26	
p(T<=t) Value of Paired-t Test	4.86657E-08	

5. CONCLUSION & FUTURE WORK

In this paper, we have demonstrated that automatic medical image segmentation method using independent component analysis. Futhermore we evaluated this method comparing with general thresholding method and evaluated using probability of error and ultimate measurement accuracy with test data. For the test data all of the results are close to gold standard. The segmentation method using independent component analysis has a "True Positive Rate" of over 95 percent and a "False Positive Rate" of 1 percent. The mislabelling rate is near 1 percent. It means that the automatic method demonstrated in this dissertation has a good result. The segmentation method using independent component analysis offer several distinct advantages over other segmentation. First, before the segmentation there's no need to know a priori informations about the region to be segmented. Second, independent component analysis method gives good spatial resolution result compare to general threshold method and using this method the detail part of the region in medical images were discriminated. Finally, the medical image segmentation technique is the start of the 3-dimensional medical image reconstruction technique and that is used for diagnosis, treatment, preoperative planning, and outcomes simulation for various interventional options but the bad result of segmentation is one of the major obstacles. The segmentation method described in this dissertation efficiently segment detailed part of medical image and it can be improve 3-dimensional medical image reconstruction technique.

Independent component analysis has many application areas like blind separation of electroencephalographic and magnetoencephalographic data, feature extraction and the analysis of natural images. Especially, blind source separation can be applied to the noise reduction from the biomedical signals, for example, ocular noise and 60Hz artifact extraction from EEG, fetal monitoring signal analysis, EKG signal analysis, etc. Independent component analysis relies on several model assumptions which can be applied to each case described above. The assumptions may be inaccurate or even incorrect. Finding and making suitable model assumption will be interesting research area.

REFERENCES

[1] G. Wang, M. W. Vannier, M. W. Skinner, W. A. Kalender, A. Polacin and D. R. Ketten, "Unwrapping cochlear implants by spiral CT," IEEE Transactions of Biomedical Engineering, vol.43, no.9, pp.891-900, 1996

[2] H. L. Seldon, "Three-dimensional reconstruction of temporal bone from computed tomographic scans on a personal computer," Arch. Otolaryngol. Head Neck Surg., vol.117, pp.1158-1161, 1991

[3] H. Takahashi and I. Sando, "Computer-aided 3-D temporal bone anatomy for cochlear implant surgery," Laryngoscope, vol.100, pp.417-421, 1990

[4] R. Frankenthaler, V. Moharir, R. Kikinis, P. V. Kipshagen, F. Jolesz, C. Umans, and M. P. Fried, "Virtual Otoscopy, Computers in Otolaryngology," vol.31, pp.383-392, 1998

[5] S. K. Yoo, G. Wang, J. T. Rubinstein, M. W. Skinner and M. W. Vannier, "Three-dimensional modelling and visualization of the cochlea on the internet," IEEE Tran. Info. Tech. in Biomed., June, 2000

[6] T. Himi, A. Kataura, M. Sakata, Y. Odawara, J. Satoh, and M. Sawaishi, "Three-dimensional imaging of the temporal bone using a helical CT scan and its application in patients with cochlear implantation," ORL; Journal of Oto-Rhino-Laryngology & its related specialties, vol.58, pp.298-300

[7] C. Yuan, E. Lin, J. Millard, and J. Hwang, "Closed contour edge detection of blood vessel lumen and outer wall boundaries in black-blood MR images," Magnetic Resonance Imaging, vol.17, no.2, pp.257-266, 1999

[8] A. J. Bell and T. J. Sejnowski, "Edges are the 'independent components' of natural scenes," In Advances in neural information processing systems 9, pp.831-837, Cambridge: MIT Press, 1997

[9] A. J. Bell and T. J. Sejnowski, "The 'independent components' of natural scenes are edge filters," Vision Research, vol.37, no.23, pp.3327-3338, 1997

[10] A. J. Bell and T. J. Sejnowski, "An information-maximization approach to blind separation and blind deconvolution," Neural Computation, vol.7, no.6, pp.1129--1159, 1995

[11] Te-Won Lee, Independent Component Analysis: Theory and Applications, Kluwer Academic Publishers, 1998

[12] P. Comon, "Independent component analysis - a new concept?" Signal Processing, vol.36, pp.287-314, 1994

[13] J. P. Nadal and N. Parga, "Non-linear neurons in the low noise limit: a factorial code maximizes information transfer," Network, vol.5, pp.565-581, 1994

[14] D. J. Field, "What is the goal of sensory coding?" Neural Computation, vol.6, pp.559-601, 1994

[15] Y. J. Zhang, "A survey on evaluation methods for image segmentation," Pattern Recognition, vol.29, no.8, pp.1335-1346, 1996

[16] A. M. Nazif and M. D. Levine, "Low level image segmentation: an expert system," IEEE Trans. PAMI-6, pp.555-577, 1984

[17] J. S. Weszka and A. Rosenfeld, "Threshold evaluation techniques," IEEE Trans. SMC-8, pp. 622-629, 1978
[18] S. U. Lee, S. Y. Chung and R. H. Park, "A comparative performance study of several global thresholding techniques for segmentation," CVGIP, vol.52, pp.171-190, 1990
[19] J. Liu and Y. H. Yang, "Multiresolution Color Image Segmentation," IEEE Trans. on Pattern Analysis and Machine Intelligence, vol.16, no.7, 1994

저 자 소 개

배 수 현(裵 秀 賢)

1969년 3월 8일 생. 1996년 연세대 전기공학과 졸. 1998년 동대학원 생체공학과(석사). 2001년 동대학원 생체공학과(박사).

유 선 국(兪 善 國)

1959년 1월 8일 생. 1981년 연세대 전기공학과 졸. 1983년 동대학원 전기공학과(석사). 1989년 동대학원 전기공학과(박사). 1990-1995 순천향대 전기공학과 전임강사, 조교수. 1998-2000 The University of Iowa Visiting Associate. 1995-현재 연세대학교 의학공학교실 조교수, 부교수

김남현(金 南 鉉)

1954년 8월 30일 생. 1977년 연세대 전기공학과 졸. 1982년 동대학원 전기공학과(석사). 1987년 동대학원 전기공학과(박사). 1988-현재 연세대학교 의학공학교실 전임강사, 조교수, 부교수